Molecular Vision 2023; 29:365-377 <http://www.molvis.org/molvis/v29/365>
Received 30 January 2023 | Accepted 20 December 2023 | Published 26 December 2023

Distribution of *TGFBI* variants in patients with early onset glaucoma

Viney Gupta,[1] Arnav Panigrahi,[1] Bindu I. Somarajan,[1] Shikha Gupta,[1] Koushik Tripathy,[1] Abhishek Singh,[1] Anshul Sharma,[2] Radhika Tandon,[1] Dibyabhaba Pradhan,[3] Arundhati Sharma,[2] Tushar Kushwaha,[4] Krishna K. Inampudi[4]

[1]Dr Rajendra Prasad Centre for Ophthalmic Sciences, All India Institute of Medical Sciences, New Delhi; [2]Department of Anatomy, All India Institute of Medical Sciences, New Delhi; [3]Department of Biomedical Informatics, Indian Council of Medical Research, New Delhi; [4]Department of Biophysics, All India Institute of Medical Sciences, New Delhi

Purpose: To describe a novel association of *TGFBI* variants with congenital glaucoma in a family with GAPO (growth retardation, alopecia, pseudoanodontia, and progressive optic atrophy) syndrome, as well as among other unrelated cases of juvenile onset open-angle glaucoma (JOAG) and primary congenital glaucoma (PCG).
Methods: This study of one family of GAPO with congenital glaucoma and three unrelated patients with JOAG analyzed a common link to glaucoma pathogenesis. Three girls with GAPO syndrome born to consanguineous parents in a multi-generation consanguineous family were identified. Two of the girls had congenital glaucoma in both eyes, while the elder sibling (a 10-year-old female) had features of GAPO syndrome without glaucoma.
Results: A genetic evaluation using whole exome sequencing revealed a novel homozygous *ANTXR1* mutation in all three affected siblings with GAPO. No other mutations were detected in the genes associated with glaucoma. A rare missense variant in the *TGFBI* gene was shared in the two siblings with congenital glaucoma and GAPO syndrome. We found three other unrelated patients with JOAG and one patient with primary congenital glaucoma with no known glaucoma causing gene mutations, but having four different missense variants in the *TGFBI* gene. One of these patients with JOAG had familial granular corneal dystrophy. Molecular dynamic simulations of TGFBI and 3-D structural models of three of its variants showed significant alterations that could influence TGFBI protein function.
Conclusions: The possibility that variations in the *TGFBI* gene could have a possible role in the pathogenesis of congenital and juvenile onset open-angle glaucomas needs further evaluation.

Primary congenital glaucoma (PCG; OMIM 231300) and juvenile onset open-angle glaucomas (JOAG) are generally monogenic, with genes having a strong biologic effect that plays a role in their pathogenesis. Along with *MYOC, CYP1B1* and *LTBP2* [1-7], newer genes associated with either form of glaucoma include the *CPAMD8*, *GPATCH,* and *EFEMP1* [8-10]. However, a large number of PCG and JOAG patients do not have a known mutations in any of these genes [11], indicating that chromosomal loci harboring putative genes associated with PCG and JOAG remain to be discovered [12]. The advent of next-generation sequencing now offers the opportunity for new gene discoveries, especially for diseases where genetic variations have a significant biologic effect on disease causation.

One of these genetic diseases is growth retardation, alopecia, pseudoanodontia, and progressive optic atrophy (GAPO; OMIM 230740) syndrome, an extremely rare genetic disorder, with only about sixty cases reported to date. The ocular features of GAPO syndrome include puffy eyelids, sparse eyelash hair, poliosis, hypertelorism, ptosis, strabismus, nystagmus, megalocornea, keratoconus, keratopathy, optic atrophy, myelinated retinal nerve fiber layer, and congenital glaucoma (buphthalmos) [13]. The diagnosis of GAPO is usually made early due to the characteristic premature "geriatric" appearance of the patients and the presence of cardinal features like alopecia and pseudoanodontia, as well as the associated features like dwarfism, prominent supraorbital ridges, frontal bossing depressed nasal bridge, long philtrum, and a wide open anterior fontanelle. Late onset alopecia has also been frequently documented [14,15]. Patients with GAPO have a reduced life span and usually die in their third or fourth decades of life due to generalized interstitial fibrosis of the lungs and atherosclerosis [16,17].

The invariable consanguinity in families with GAPO points toward an autosomal recessive mode of inheritance caused by mutations in *ANTXR1* at chromosomal position 2p14; this gene codes a protein essential for intracellular actin assembly [18,19]. Defective production of this protein alters cell adhesion properties, leading to excessive deposition of

Correspondence to: Viney Gupta, Dr Rajendra Prasad Centre for Ophthalmic Sciences, All India Institute of Medical Sciences, New Delhi, Delhi-110029, India; Phone: +911126593003; email: gupta_v20032000@yahoo.com

extracellular matrix (ECM) secondary to reduced turnover and resulting in the various phenotypic features characteristic of this syndrome [19,20]. While the occurrence of glaucoma is reported among patients with GAPO syndrome [17,21-25], whether glaucoma develops due to mutations in the *ANTXR1* gene itself or in some other (glaucoma-associated) genes is unknown.

This report analyses the genetic background of two of three sibling children with GAPO syndrome who also had congenital glaucoma. Whole exome sequencing (WES) analysis pointed toward a Transforming Growth Factor Beta Induced (*TGFBI*) gene variant common to both siblings. We found other *TGFBI* variants in three unrelated patients with JOAG, one of whom had familial granular corneal dystrophy, and in one patient with PCG.

METHODS

Four girls from a multigenerational consanguineous family presented to us. Three of the girls were affected with GAPO, and two also had congenital glaucoma in addition to GAPO features (Figure 1). The family resided in North India, where a strong tradition of consanguinity persists. The three cases in the family described here are the three girls with features of GAPO syndrome.

Case 1 (Proband): A 4-year-old girl, born of consanguineous parents, presented with complaints of watering and an asymmetric corneal enlargement of the right eye (RE). A physical examination revealed progressive frontal alopecia with a receding hairline, frontal bossing, high forehead, prominent supraorbital ridges, depressed nasal bridge, anteverted nostrils, long philtrum, umbilical hernia, sparse eyebrows,

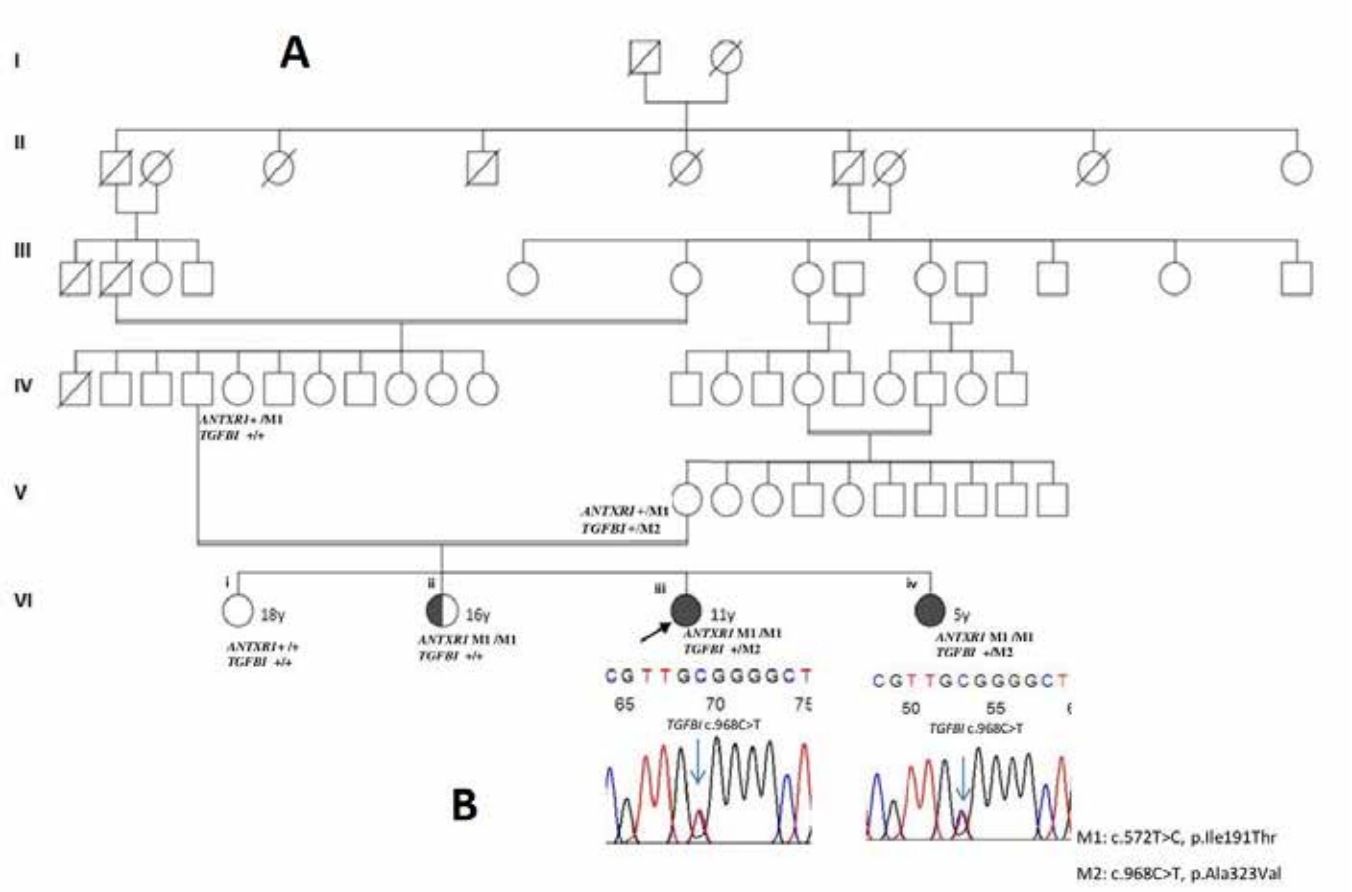

Figure 1. Pedigree and chromatogram. **A**: Pedigree chart of the family with three children affected with GAPO syndrome showing three generations of consanguinity. The half shaded circle depicts the child having only GAPO syndrome but not glaucoma. The younger two siblings who had glaucoma with GAPO syndrome are depicted as full shaded circles. The ages mentioned in the pedigree are those at their last follow up. . "+/+ indicates homozygous wild genotype and +/M1 indicates heterozygous *ANTXR1* p.Ile191Thr genotype and +/M2 indicates heterozygous *TGFBI* p.Ala323Val mutation. **B**: Chromatograms showing a heterozygous, *TGFBI;*NM_000358.3:c.968C>T; p.Ala323Val mutation in the proband and younger sibling who had both congenital glaucoma and GAPO syndrome.

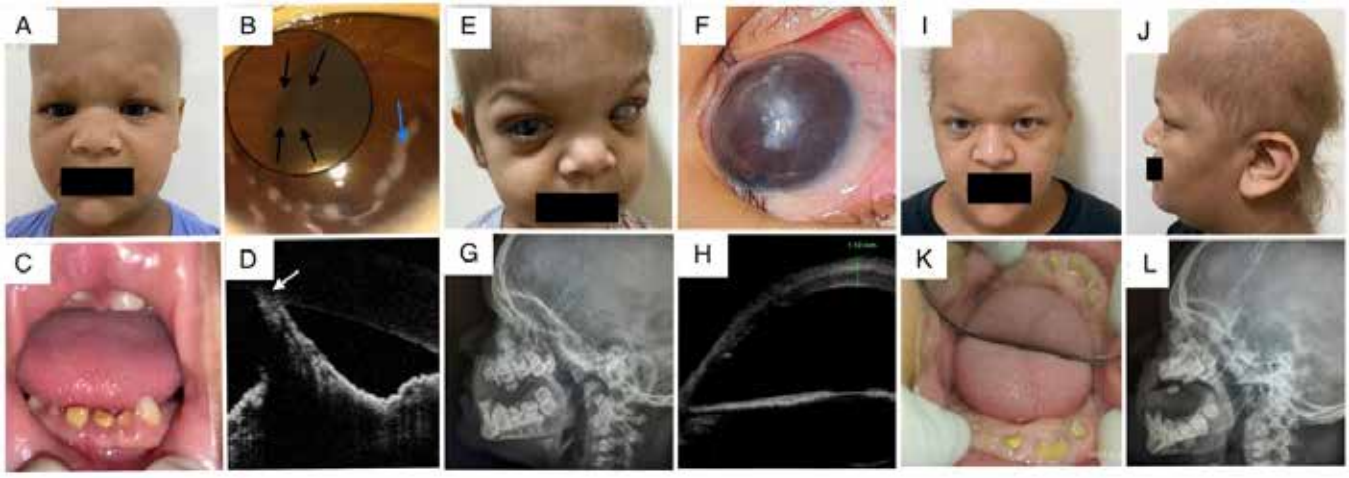

Figure 2. Clinical photographs of Case 1 (A-D), Case 2 (E-H), and Case 3 (I-L). Front facial profile and side facial profile of the patients illustrate the presence of a characteristic geriatric appearance, with alopecia, sparse eyebrows, frontal bossing, prominent supraorbital ridges, depressed nasal bridge, anteverted nostrils, and a long philtrum. Clinical photograph of the oral cavity shows impaction of teeth, with a reduction in tooth number. Radiograph of the face (lateral view with open mouth) reveals a normal number of teeth, confirming pseudoanodontia. Anterior segment photograph of Case1 (B) reveals the presence of megalocornea with prominent iridocorneal adhesions and keratopathy (blue arrow). Corneal opacities are also seen (black arrows; magnified inset). AS-OCT image of the same patient (D) confirms the iridocorneal adhesions (white arrow). Central keratopathy can be seen in the anterior segment photograph of RE of Case 2 (F). An ultrasound biomicroscopy (UBM) of the same patient revealed central corneal thickening with a thinned out iris and ciliary body (H).

and an appearance of premature aging (Figure 2A-D). An oral examination revealed the absence of a regular dentition pattern (Figure 2C), and a radiograph of the teeth revealed impacted dentition, confirming pseudoanodontia. Her weight (12 kg) and height (92 cm) were below the 3rd percentile. The patient's mental status was normal, and she showed no developmental delay.

Examination under anesthesia (EUA) revealed enlarged corneal diameters, an IOP of 30 mmHg, with corneal edema precluding a detailed anterior and posterior segment evaluation in RE. Her left eye (LE) had a clear cornea with an IOP of 16 mmHg. The patient underwent RE trabeculectomy with mitomycin. An anterior segment evaluation during a subsequent EUA (post-operatively), when the cornea had cleared up, revealed the presence of Haab's striae and peripheral keratopathy with irido-corneal adhesions that were seen on an ASOCT examination in RE (Figure 2B,D). Her optic disc examination showed a vertical cup disc ratio (CDR) of 0.4:1, with temporal disc pallor in RE; while LE showed a healthy disc with a CDR of 0.2:1. Eventually, three years after the RE surgery, she developed increased IOP in her LE and underwent LE trabeculectomy with mitomycin. Her IOP has been controlled in both eyes (BE) since then.

An abdominal ultrasound revealed the presence of normal kidneys and ovaries. An MRI of the brain did not reveal any intracranial abnormality. Other investigations were normal, including complete blood counts, serum and urine biochemistry, hormonal assays, and echocardiography,.

Case 2: The younger sibling of the proband presented at 1 year of age with complaints of watering BE. She had lush black hair until six months of age, followed by progressive hair loss. She had a prominent supraorbital ridge, depressed nasal bridge, high forehead, wide anterior fontanelle, and a prematurely aged look (Figure 2E-H). She also had pseudoanodontia. Like her elder sister, she had growth retardation, with her weight and length below the 3rd percentile for her age.

An EUA revealed BE horizontal corneal diameter of 13.5 mm, along with the presence of a diffuse corneal haze in LE. She also had a central keratopathy in RE (Figure 2F). Her IOP was 28 mmHg in RE and 32 mmHg in LE. An ultrasound biomicroscopy (UBM) examination revealed central corneal thickening and a thinned out iris and ciliary body (Figure 2H). She had a cup disc ratio of 0.6:1 in BE. She underwent BE trabeculectomy with ab externo trabeculotomy with mitomycin. The surgery was uneventful, and she maintained a normal IOP till her last follow up.

Case 3: The 10-year-old elder sister of the proband was also evaluated for GAPO features. She was observed to have all the phenotypic features of this syndrome (Figure 2I-L). Her height (120 cm) and weight (20 kg) were below the third centile for her age. She had no developmental delay. Her

visual acuity was 6/6 in both eyes, and her IOP was RE 14 mmHg and LE 16 mmHg. Her corneas were clear, and gonioscopy revealed wide open angles without any abnormality. Her optic nerves were normal.

Whole exome sequencing: Blood samples were withdrawn from the four children, the parents, and the paternal grandmother after informed consent was obtained from the parents of the children. The study was performed according to the tenets of the Declaration of Helsinki, and ethics committee approval was obtained from our institute's ethics committee. Signed informed consent according to the guidelines of our institute's ethics committee was obtained.

Genomic DNA was extracted from peripheral blood for genetic evaluation. WES capture was performed using the Sure Select Clinical Research Exome V2 kit (Agilent Technologies, Santa Clara, CA). Variant analysis was performed using the GenomeAnalysisTK-3.6 toolkit. The generated variant call files (VCFs) were analyzed using Golden Helix VarSeq Software v.1.2.1 (Bozeman, MT). VarSeq variants with read depth <15 and genotype quality score <20 were excluded. Rare mutations were identified using variant frequency databases to remove variants present at high frequencies among large population groups. The remaining variants were filtered according to minor allele frequency (MAF)<0.001 in multiple databases, including Exome Aggregation Consortium (ExAC), 1000 Genomes Project and gnomAD.

Variants, specifically in the two sisters with glaucoma, were filtered based on only those exonic variants that were non-synonymous missense variants, frameshifts and indels, and splice region variants and were absent among 50 ethnically and geographically matched healthy controls. Inherited variants that were present in both the affected sisters with congenital glaucoma and one of the parents were also examined for any association with known glaucoma genes.

Copy number variant (CNV) analysis was performed to look for CNVs in the known genes for glaucoma or others with a strong association with glaucoma pathogenesis. The CNVs were annotated with RefSeq gene annotations and Database of Genomic Variants v107. The CNVs were then classified to assess their pathogenicity using classify CNV (a software tool for clinical annotation of copy-number variants). The CNVs common in both affected individuals were visually inspected using integrative genomic viewer (IGV).

We used homozygosity mapping to identify long stretches of homozygous haplotypes in genes associated with glaucoma. Regions of homozygosity (ROHs) were identified using the AutoMap software (Quinodoz et al.) on the WES data [26].

The WES data of a cohort of 40 patients with JOAG, obtained by following the standard data analysis for identifying variants, was used to look for the presence of identified genes in the two sisters with both GAPO syndrome and glaucoma. All 40 patients with JOAG had been screened for non-synonymous missense variants, frameshifts and indels, and splice region variants in the known glaucoma genes that were absent among the 50 healthy controls

The variants identified in *TGFBI* in the family with GAPO were confirmed by Sanger sequencing. Primers flanking the variant sites were determined and genomic DNA was amplified in the proband and siblings. The PCR product was cleaned and analyzed on Applied Biosystems-Genetic Analyzer (ABI 3730XL sequencer; Applied Biosystems/LifeTechnologies, Carlsbad, CA). To confirm the variant, the Unipro UGENE program was used to manually analyze the Sanger sequencing data.

In silico 3D-modeling and molecular dynamic analysis of TGFBI and its variants: The nucleotide sequence of the TGFBI protein was retrieved from NCBI (ID), and the structure was modeled through comparative modeling using the Robetta server [27].The structure of full-length TGFBI was modeled using the coordinates of PDBID:5NV6 [28]. For further refinement, the model was subjected to a molecular dynamics (MD) simulation for 200 ns. The refined structure was validated using MolProbability Server [29]. The last frame of the 200ns simulation was used as a template for modeling the mutant forms of TGFBI, including A323E, A323V, and the 649 frameshift. The modeled mutants were then simulated for 200 ns each to understand the impact of variations on the structure and dynamics of the TGFBI protein.

MD simulations of the modeled proteins were conducted using GROMACS software version 2021.5 [30]. The CharmM36 forcefield was used to generate the topology, and the system was solvated using the TIP3P water model [31]. The system was neutralized by the addition of the appropriate number of sodium ions. System equilibration was then performed under successive NVT and NPT ensembles for 500 ps each. The production simulation was run using a leap-frog dynamics integrator and a step size of 2 fs with consideration of the periodic boundary conditions in all three dimensions. The trajectory was analyzed to obtain various parameters, such as the RMSD (Root Mean Square Deviation), RMSF (Root Mean Square Fluctuation) and Rg (Radius of Gyration), to assess the structural changes in TGFBI protein in its mutant and native forms. Using MD trajectory, principal

component (PC) analysis was performed to understand the global motions of the TGFBI protein and its three mutant forms. The covariance matrix was generated from the Cα atom coordinates and diagonalized to obtain the eigenvectors. Since the first two eigenvectors described the major proportion of the trace of the covariance matrix, the trajectory was projected along the first two principal components. A free energy landscape was generated using the 2-dimensional projection of the trajectory along PC1 and PC2.

RESULTS

We found a missense homozygous *ANTXR1* gene mutation; (NM_032208.2:c.572T>C, p.Ile191Thr) in all three children affected with GAPO. This change was deemed novel and disease causing by mutation taster (0.99), PolyPhen-2 (1.0), and PROVEAN (−4.0). It is classified as a variant of uncertain significance as per ACMG guidelines. Another change at this position, c.572T>G, p.Ile191Ser is reported in the COSMIC database (COSV100362660).

Homozygosity mapping applied to the WES data of the consanguineous family detected one large (11Mb) homozygous region involving the *TEK* gene (i.e., chromosome 9) in only one of the two sisters with congenital glaucoma, among the genes known for glaucoma. However, no CNVs or intronic splice region variants were detected in the *TEK* gene in either of the sisters.

No missense variants (as per ACMG criteria) or CNVs were detected that co-segregated with glaucoma in the two girls with congenital glaucoma (Cases 1 and 2) at any of the known loci for Mendelian forms of glaucoma (GLC1A, GLC1B, GLC1D-Q) or PCG (GLC3A-D), including the known causative genes, *MYOC* (GLC1A), *CYP1B1*(GLC3A), *WDR36* (GLC1G), *ASB10* (GLC1F), *OPTN* (GLC1E), *NTF4* (GLC1O), *TBK1*(GLC1P), *LTBP2* (GLC3C), *FOXC1, PITX2*, *TEK, COL4A1,* and *PAX6.*

Three missense variants in *PTPN4*, *PCDHB4* and *GGT2,* were observed exclusively in the two sisters with GAPO and congenital glaucoma (case 1 and case 2; Appendix 1**).** The variants of *PTPN4* and *PCDHB4* were rejected as causal because of the absence of any association in glaucoma pathogenesis pathways. The *GGT2* variant was also not considered as it was earlier reported that hGGT2 does not encode a functional enzyme and therefore is unlikely to play a role in glaucoma pathogenesis [32]. By contrast, the *TGFBI* is known to have a strong role in ocular anterior segment development [33], and a missense heterozygous variant in *TGFBI*, 5–135388650-C-T NM_000358.3:c.968C>T NP_000349.1:p.Ala323Val (Figure 1A) was found. While this variant is likely benign according to the ACMG criteria, the LoF score for this variant (0.132) is suggestive of it being possibly damaging. The variant is highly conserved, with a genomic evolutionary rate profiling (GERP) value of 5.65. The *Clinvar* (RCV000279769.3) star rating score extracted for the variant was 1/4 with two submissions, benign, and uncertain significance for corneal dystrophy.

We then looked for the presence of *TGFBI* gene variants in a cohort of 40 patients with JOAG (diagnosed before 25 years of age) in whom WES had previously been done. We found two *TGFBI* variants present in two unrelated patients with JOAG. Both patients had nonfamilial glaucoma diagnosed before the age of 40 years. Neither had any other mutations (either in exonic or intronic regions) of significance in the known glaucoma genes. In one patient, a *TGFBI* heterozygous missense variant was found in the same codon as observed in the described cases of GAPO, but with a different amino acid residue; 5–135388650-C-A; NM_000358.3:c.968C>A, NP_000349.1:p.Ala323Glu. The second patient with JOAG had a novel null variant (frameshift mutation) 5–135397226-C-; NM_000358.3:c.1944del, NP_000349.1:p.Ser649LeufsTer22. Both patients had a normal anterior segment with a clear cornea. None of their family members were reported to have any ocular disorders.

A third patient with JOAG had concomitant granular corneal dystrophy (GCD) and had a heterozygous *TGFBI* mutation NM_000358.3:c.1663C>T, NP_000349.1:p.Arg555Trp, which is reported as pathogenic in *Clinvar (VCV000007866.7)* with 3 submissions associated with GCD (Table 1). We looked for other mutations or CNVs in the known genes for glaucoma, but we did not find any. The patient had an untreated IOP of 30 mmHg in BE with advanced glaucomatous optic atrophy. This patient had 2 other first degree relatives (a brother and his daughter) also affected with GCD but without having glaucoma or raised IOP (Figure 3). The clinical features of these three patients with JOAG are given in Table 2. However, the clinical features did not differ from those of other JOAG patients.

We also found a *TGFBI* variant (likely pathogenic according to ACMG) in another PCG patient. Of 15 unrelated patients with PCG who underwent WES, we found that this patient with congenital glaucoma had a rare *TGFBI* variant and no other associated known glaucoma gene mutation (Table 1).

A comparative modeling of the TGFBI variants in this study (p.Ala323Val, p.Ala323Glu and p.Ser649LeufsTer22) was performed since the available crystal structures lack the C-terminus (Figure 4). The model was subjected to a 200 ns MD simulations for refinement. During this simulation, the C-terminal region of the protein was gradually stabilized

Molecular Vision 2023; 29:365-377 <http://www.molvis.org/molvis/v29/365>

Table 1. *TGFBI* variants identified in Congenital glaucoma and JOAG patients.

Subjects	Variant	rs number	Transcript HGVS coding	Amino acid change	gnomAD South Asian frequency	ACMG Classification	Clinical significance
Case 1 & Case 2 GAPO with glaucoma	5:135388650-C-T	rs201210696	NM_000358.3:c.968C>T	p.Ala323Val	0.0007	BS1, BS2,BP4	Likely Benign
JOAG	5:135388650-C-A	rs201210696	NM_000358.3:c.968C>A	p.Ala323Glu	0.0000326	PM2	US
JOAG	5:135397226-C-	-	NM_000358.3:c.1944del	p.Ser649LeufsTer22	NA	PM2	US
JOAG with GCD	5:135392469-C-T	rs121909208	NM_000358.3:c.1663C>T	p.Arg555Trp	0.0002070	PP5,PM1,PM5, PM5,PM2, PP3	Pathogenic
PCG	5:135382607-T-C	-	NM_000358.3:c.527T>C	p.Val176Ala	NA	PP3	Likely Pathogenic

ACMG: American College of Medical Genetics US: Uncertain Significance NA: not available GAPO: Growth retardation, alopecia, pseudoanodontia, and progressive optic atrophy JOAG: Juvenile onset open angle glaucoma GCD: Granular corneal dystrophy PCG: Primary congenital glaucoma.

through interactions with the FAS1–4 and FAS1–3 domains. The last frame of the simulation was used as a template to generate TGFBI variants A323E, A323V, and 649 frameshift, which were then subjected to MD simulations to understand the effect of the mutations on the local and global structure of TGFBI and its variants. Analysis of the MD trajectory yielded various parameters, such as the root mean square deviation (RMSD), root mean square fluctuation (RMSF) and radius of gyration (RG), which allow assessment of structural deviation, residue fluctuations, and compactness of the proteins, respectively (Appendix 2). The MD simulations were followed by Principal Component Analysis (PCA) to study the overall motions of the TGFBI and these 3 variants. PCA extracts correlated motions of the protein from the MD trajectory, thereby allowing us to study the impact of mutations on distant regions of the protein and subsequent changes in protein movement. Projection of the trajectory along PC1 and PC2 depicted correlated motions of various domains of the protein, as shown in Appendix 3. We found that TGFBI fluctuated between an elongated and a banana-like shape due to bending between the FAS1–2 and FAS1–3 domains. The bending movement was more prominent in all variants compared to wild-type (WT) TGFBI, and occurred majorly in the FAS1–2 and FAS1–3 domains. The free energy landscape (FEL) was also generated to visualize the potential energy of TGFBI and mutants. The impact of the three variants was also evident on the FEL, since the free energy wells were shallow and distorted compared to the deeper well of the WT TGFBI (Figure 5).

DISCUSSION

This family of three children affected with GAPO, two of whom presented with bilateral congenital glaucoma, allowed us to study the genetic association of glaucoma with GAPO syndrome. All three carried a novel missense homozygous *ANTXR1* gene mutation.

Glaucoma with GAPO syndrome has been reported in ten cases to date [14,15,17,20-25]. Glaucoma in five of these patients was early onset open angle glaucoma [14,15,24,25]. Primary congenital glaucoma (PCG) is described in five patients [17,21-25], and asymmetric glaucoma, as seen in Case 1 of the GAPO family that presented to us, has also

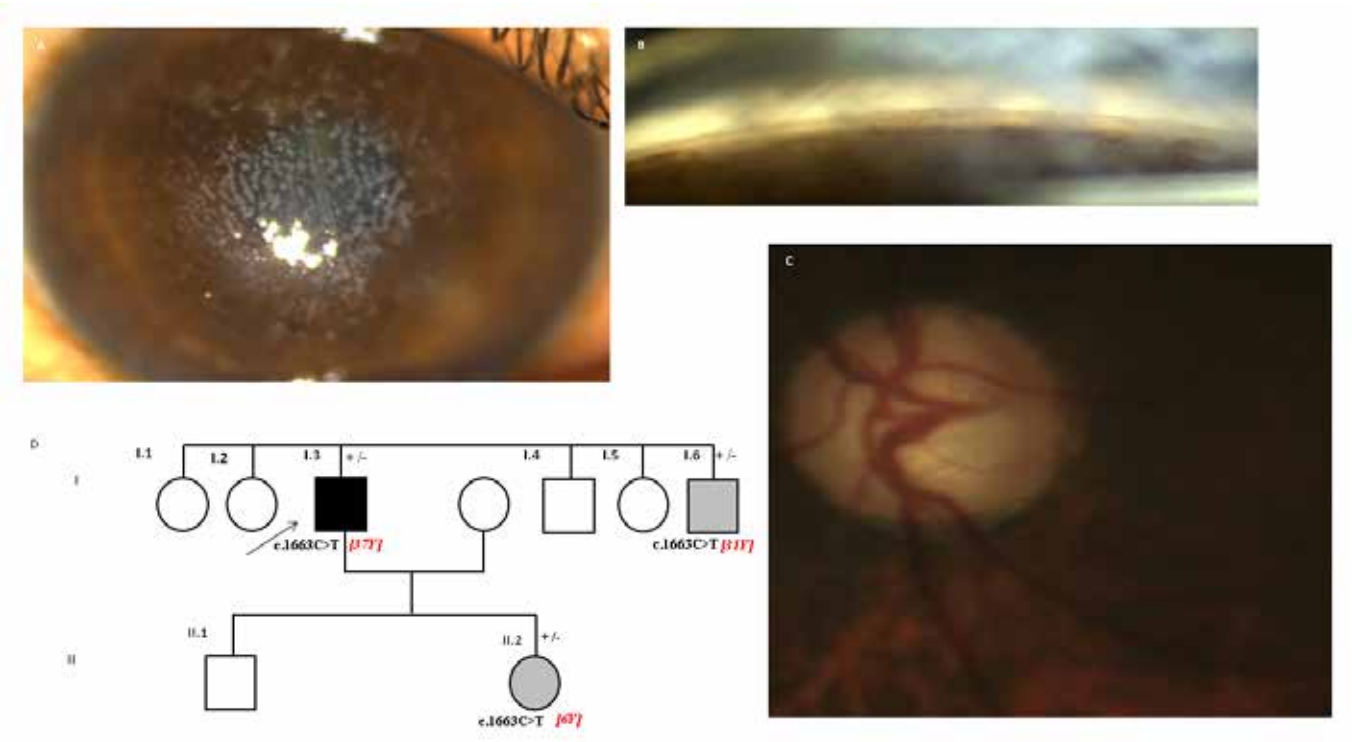

Figure 3. Clinical photographs of patients with JOAG and corneal dystrophy. **A**: Anterior segment photo of the patient showing granular corneal dystrophy. **B**: Goniophotograph showing open angles. **C**: Fundus photograph of the patient showing advanced glaucomatous optic atrophy. **D**: Pedigree chart of the patient. Black shaded square depicts the proband having glaucoma and granular dystrophy. Grey shaded square and circle indicates affected status with only granular corneal dystrophy. The ages mentioned in the pedigree are those at the patients' last follow up.

Table 2. Clinical features of patients with Glaucoma (without GAPO) harbouring *TGFBI* variants.

Subjects	TGFBI Variant	Age of onset/ Gender	Untreated IOP (mmHg) RE, LE	Cup disc ratio RE, LE	Snellen visual acuity RE, LE	Mean Deviation (dB) on visual field RE, LE
JOAG	5:135388650-C-A	38/F	41, 37	0.8, 0.9	6/12, 6/60	−24, NA
JOAG	5:135397226-C-	19/F	28,26	0.7, 0.8	6/6, 6/60	−25, −35
JOAG with GCD	5:135392469-C-T	35/M	30,30	0.8, 0.9	6/60, 6/36	Only central 5 degree
PCG	5:135382607-T-C	5 months/M	30,32	0.6, 0.8	NA	NA

JOAG: Juvenile onset open angle glaucoma GCD: Granular corneal dystrophy PCG: Primary congenital glaucoma NA: Not available

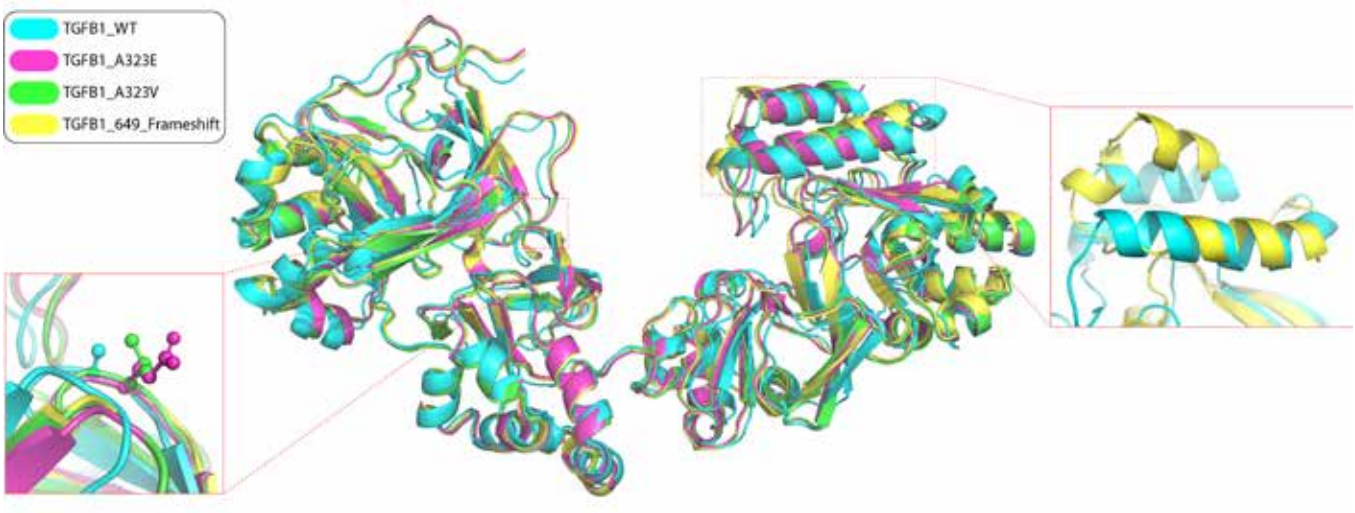

Figure 4. Modeled structures of the full-length TGFBI protein and its variants are depicted in cartoon representation. The residue substitution at 323 position is magnified along with the C-terminal helices in wild-type and 649 frameshift TGFBI.

been documented [17,21], while others have described a late presentation with end stage glaucoma [21,22,25]. The pathogenesis of congenital glaucoma in children with GAPO syndrome is not clearly understood. If mutations in the *ANTRX1* gene are postulated as a cause of glaucoma in GAPO, then this does not explain why so few patients with GAPO develop glaucoma and why only 2 of the 3 siblings with the *ANTRX1* mutation in the family described by us developed glaucoma. A variable expression of *ANTRX1* mutation could be one reason why the elder sister (case 3) with *ANTRX1* mutation and GAPO syndrome did not have glaucoma. However, even if we consider a variable expressivity in *ANTRX1* as the reason for one sibling with GAPO syndrome not developing congenital glaucoma in this family, we believe the presence of the *TGFBI* variant may have a role in modification of this expression. The clinical significance of the *TGFBI* p.Ala323Val variant, although conflicting in *Clinvar*, cannot not be ruled out and its association with disease requires further investigation.

The abnormal expression of *TGFBI* is related to the occurrence and development of some types of cancers, as well as different types of corneal dystrophies, including lattice corneal dystrophies (LCD) and granular corneal dystrophies (GCD) [34]. The *TGFBI* gene was one of the first discovered to cause corneal dystrophies [35] and since then, numerous reports on genotype–phenotype correlations have been published. The human protein transforming growth factor-beta-induced protein ig-h3 (Beta ig-h3), encoded by *TGFBI,* has four FASI domains, and the mutated amino acid observed in our two patients corresponds to the FAS1–2 domain of TGFBIp. The *TGFBI* mutations associated with various corneal dystrophies are located in the FASI-1 and FASI-4 domains [36]. No association with developmental glaucoma has been noted.

The *TGFBI* gene lies within the linkage area mapped as a glaucoma locus 5q22.1-q32 [37]. A gene expression profile of human trabecular meshwork (TM) tissue by SAGE (serial analysis of gene expression) has shown a higher expression of *TGFBI,* along with other glaucoma causing genes and genes involved in typical TM maintenance functions [38]. A study by Kim et al., using Alb-hßigh3 transgenic mice, showed that overexpressed human βigh3/ (hßigh3)/ TGFBIp in the blood might be involved in anterior segment morphogenesis and eye development in mice. The phenotype observed in transgenic mice is similar to that seen in human eye disorders, such as anterior segment dysgenesis and Peters' anomaly [39]. These observations support a role for *TGFBI* in congenital glaucoma, as observed in the two sisters with GAPO. A string analysis also showed that *TGFBI* and *LTBP2* (associated with congenital glaucoma) are co-expressed, possibly interacting with *MYOC* and *CYP1B1*. Glaucoma has also been observed in a patient with a *TGFBI,* R124H mutation, though the phenotypic details of this patient are not known [40]. These observations suggest a role for *TGFBI* in glaucoma pathogenesis, in conjunction with other genes.

We also found 3 unrelated (non-dominant) patients with JOAG and one patient with PCG who had with *TGFBI* variants in a separate cohort; none of these patients had any known glaucoma gene mutations. One patients had GCD; however, two other members of his family with GCD and the *TGFBI* mutation did not have glaucoma. The differences in

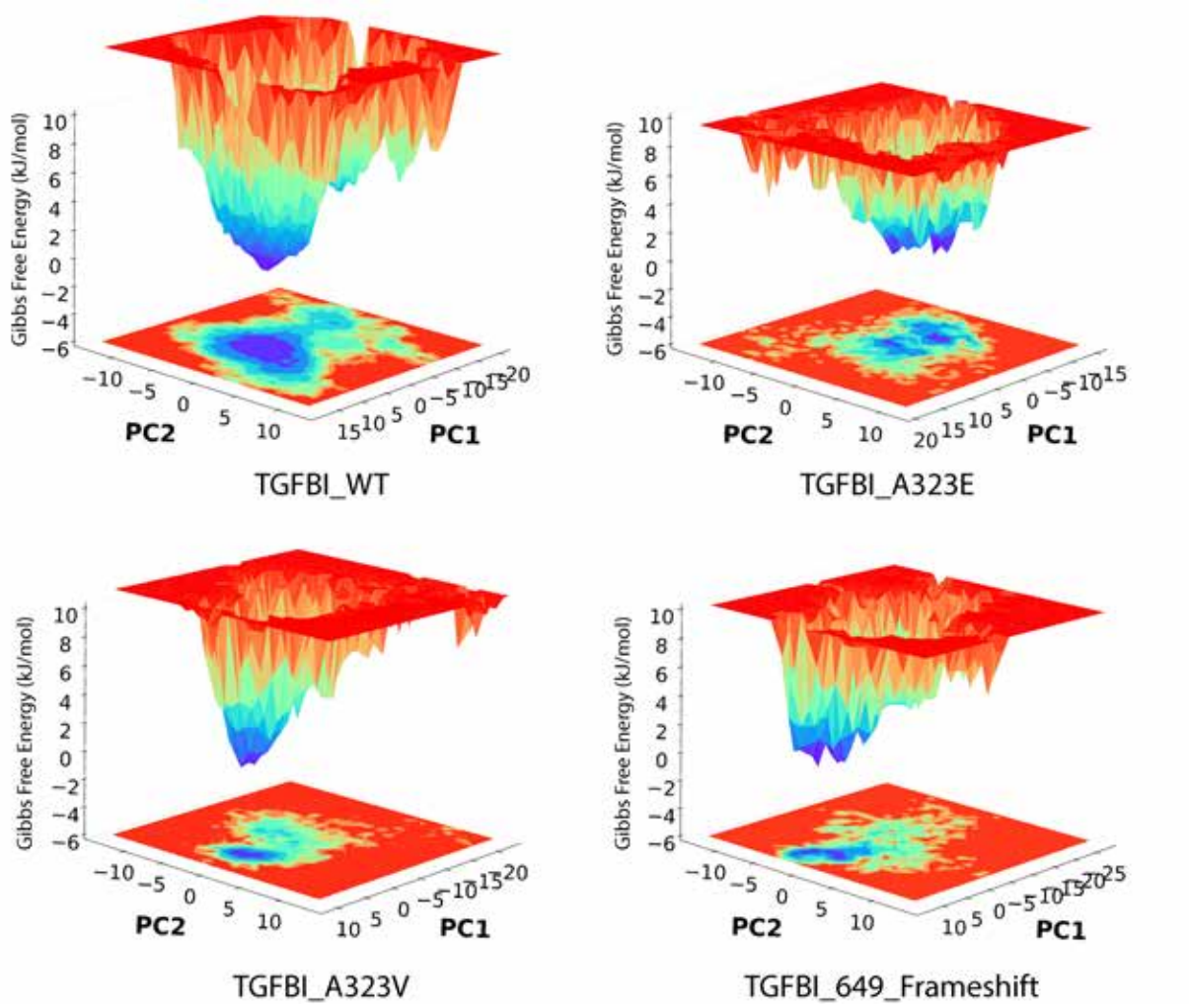

Figure 5. Free energy landscape (FEL) generated from the projection of trajectory on PC1 and PC2. The FEL was deeper for the wild-type TGFBI compared to the shallow FELs of the mutant forms due to decreased stability of the protein.

phenotypic expression among family members in this family with GCD and with the same *TGFBI* mutation may also reflect differences in genetic background/modifier alleles that might affect the expression of *TGFBI* co-regulators. No report in the literature has described an association between JOAG and GCD, and the finding of the *TGFBI* mutation leads us to postulate that variations in this gene could be contributing to glaucoma pathogenesis.

These 6 patients with early onset glaucoma and having variants in the same *TGFBI* gene support a role for *TGFBI* in glaucoma pathogenesis. A high degree of phenotypic variability and incomplete penetrance is known for *TGFBI* mutations; however, the fundamental reason why different gene variations cause morphologically distinct phenotypes remains elusive.

The modeling studies of the TGFBI wild-type, along with the three variants A323E, A323V, and 649-frameshift, have provided insights into the effect of these variations on the full-length structure and its dynamics. While specific aggregation mechanisms cannot be deduced at this stage, the alteration of the protein dynamics was clearly evident in the simulation studies. In this study, we built models of mutant forms of TGFBI protein and subjected them to molecular dynamics simulations (MDS), which attempt to mimic the protein's physiologic aqueous environment *in silico.* Subsequent principal component analysis (PCA) was performed on the MDS trajectory to understand the motions of the protein and its mutant forms. The altered dynamics due to the mutations can greatly change the molecular interactions, thereby affecting the normal physiologic function of the protein. The A323 is located at the interface of the CROPT and FAS1–1

domains, and perturbation at this position can alter inter-domain interactions and even global protein structure. For A323V, the presence of a hydrophobic residue of valine on the surface can destabilize the protein, and the same was observed in molecular dynamics studies. In the case of A323E, the glutamic acid was observed to form strong intra-domain interactions with K72 and N207 from the CROPT domain and FAS1–1 domain, respectively. In the case of the frameshift variant of TGFBI, the sequence at the C-terminal is greatly altered compared to the WT.

The comparative modeling studies revealed that the C-terminal region forms two alpha-helices packed against each other with hydrophobic residues, further interacting with the FAS1–4 and FAS1–3 domains. Due to the frameshift, packing of the helices was disturbed, leading to increased solvent exposure of the C-terminal tail. The structural differences observed during the simulations for TGFBI and its mutant forms were depicted using RMSD plots which show the global structural changes in protein, RMSF plots highlighting the residue-wise fluctuations, and RG plots, which measure of the compactness of the protein. The structural changes observed in these plots for the frameshift mutant were significantly distinct compared to the wild-type.

Further understanding of the motions of the proteins was obtained by performing principal component analysis (PCA). PCA extracts the correlated motions of the protein from the MD trajectory, thereby allowing us to study the impact of mutations on distant regions of the protein and subsequent changes in protein movement. The porcupine plots recapitulate the major movements of the proteins as deduced from PCA. The observed bending movement of the protein was more pronounced in the frameshift variant, while minor variations in the other mutants were observed compared to the wild-type. The free energy landscape (FEL) is deeper than the shallow FELs of the mutant forms due to decreased protein stability. This *in silico* analysis conclusively showed that the mutations destabilized the TGFBI protein and could therefore affect its function.

The limitations of our study include its small number of patients and our inability to genotype the parents and siblings of the patients with JOAG and the patient with PCG who harbored the *TGFBI* variants. Gene expression and functional studies using cell-based assays and transgenic animal models of the mutant are also needed to examine the effect of these variants on the protein and the downstream targets to establish a cause-and-effect relationship. Moreover, potential interactions between *TGFBI* and other genes in the causation of glaucoma also need to be explored. Nevertheless, based on the findings of this preliminary report, *TGFBI* may be an interesting candidate for glaucoma studies, although we cannot identify it as a cause of glaucoma based only on our present findings. More studies in a larger patient population, as well as functional studies, are needed to further elucidate its role in glaucoma pathogenesis.

APPENDIX 1. SUPPLEMENTARY TABLE 1.

To access the data, click or select the words "Appendix 1." Details of the exonic variants shared by the two sisters with GAPO and Congenital glaucoma and one of the parents.

APPENDIX 2. SUPPLEMENTARY FIGURE 1.

To access the data, click or select the words "Appendix 2". **A**: RMSD plots showing structural deviation of the wild-type and mutant TGFBI proteins **(B)** Radius of gyration plots showing compactness of the protein. **(C)** RMSF plot showing residue fluctuation throughout the 200ns simulations. Structural alterations in the frameshift variant is clearly visible in all these plots.

APPENDIX 3. SUPPLEMENTARY FIGURE 2.

To access the data, click or select the words "Appendix 3". Porcupine plots showing correlated movements of the protein throughout the 200ns simulations along PC1. The mutant forms of TGFBI were more dynamic compared to the wild-type *TGFBI*. The highlighted region in the wild-type TGFBI shows region of less movement compared to all mutants.

ACKNOWLEDGMENTS

Data Availability: Data supporting the findings of the study are available from the corresponding author (VG) on request. Author Contributions: Concept, Design: Viney Gupta, Bindu Somarajan Data Collection: Shikha Gupta, Arnav Panigrahi, Koushik Tripathi, Anshul Sharma, Abhishek Singh, Dibyabhaba Pradhan, Tushar Kushwaha, Radhika Tandon, Amit Das, Krishna K Inampudi. Manuscript editing: Arundhati Sharma, Krishna K Inampudi. Overall Responsibility: Viney Gupta Funding: This study was supported by funding from the Indian Council of Medical Research, New Delhi, India (Grant no. ISRM/12(58)/2019). Ethics approval: The study was approved by the Institute Ethics Committee, AIIMS, New Delhi, India. Conflict of interest: None of the authors have any conflict of interests.

REFERENCES

1. Abu-Amero KK, Osman EA, Mousa A, Wheeler J, Whigham B, Allingham RR, Hauser MA, Al-Obeidan SA. Screening of CYP1B1 and LTBP2 genes in Saudi families with primary

congenital glaucoma: genotype-phenotype correlation. Mol Vis 2011; 17:2911-9. [PMID: 22128238].

2. Alsaif HS, Khan AO, Patel N, Alkuraya H, Hashem M, Abdulwahab F, Ibrahim N, Aldahmesh MA, Alkuraya FS. Congenital glaucoma and CYP1B1: an old story revisited. Hum Genet 2019; 138:1043-9. [PMID: 29556725].

3. Bayat B, Yazdani S, Alavi A, Chiani M, Chitsazian F, Tusi BK, Suri F, Narooie-Nejhad M, Sanati MH, Elahi E. Contributions of MYOC and CYP1B1 mutations to JOAG. Mol Vis 2008; 14:508-17. [PMID: 18385784].

4. Chakrabarti S, Kaur K, Kaur I, Mandal AK, Parikh RS, Thomas R, Majumder PP. Globally, CYP1B1 mutations in primary congenital glaucoma are strongly structured by geographic and haplotype backgrounds. Invest Ophthalmol Vis Sci 2006; 47:43-7. [PMID: 16384942].

5. Chen Y, Jiang D, Yu L, Katz B, Zhang K, Wan B, Sun X. CYP1B1 and MYOC mutations in 116 Chinese patients with primary congenital glaucoma. Arch Ophthalmol 2008; 126:1443-7. [PMID: 18852424].

6. Gupta V, Somarajan BI, Walia GK, Kaur J, Kumar S, Gupta S, Chaurasia AK, Gupta D, Kaushik A, Mehta A, Gupta V, Sharma A. Role of CYP1B1, p.E229K and p.R368H mutations among 120 families with sporadic juvenile onset open-angle glaucoma. Graefes Arch Clin Exp Ophthalmol 2018; 256:355-62. [PMID: 29168043].

7. Saeedi O, Yousaf S, Tsai J, Palmer K, Riazuddin S, Ahmed ZM. Delineation of Novel Compound Heterozygous Variants in LTBP2 Associated with Juvenile Open Angle Glaucoma. Genes (Basel) 2018; 9:527-1-7[PMID: 30380740].

8. Ferre-Fernández J-J, Aroca-Aguilar J-D, Medina-Trillo C, Bonet-Fernández J-M, Méndez-Hernández C-D, Morales-Fernández L, Corton M, Cabañero-Valera MJ, Gut M, Tonda R, Ayuso C, Coca-Prados M, García-Feijoo J, Escribano J. Whole-Exome Sequencing of Congenital Glaucoma Patients Reveals Hypermorphic Variants in GPATCH3, a New Gene Involved in Ocular and Craniofacial Development. Sci Rep 2017; 7:46175-1-17[PMID: 28397860].

9. Mackay DS, Bennett TM, Shiels A. Exome Sequencing Identifies a Missense Variant in EFEMP1 Co-Segregating in a Family with Autosomal Dominant Primary Open-Angle Glaucoma. PLoS One 2015; 10:e0132529[PMID: 26162006].

10. Siggs OM, Souzeau E, Taranath DA, Dubowsky A, Chappell A, Zhou T, Javadiyan S, Nicholl J, Kearns LS, Staffieri SE, Narita A, Smith JEH, Pater J, Hewitt AW, Ruddle JB, Elder JE, Mackey DA, Burdon KP, Craig JE. Biallelic CPAMD8 variants are a frequent cause of childhood and juvenile open-angle glaucoma. Ophthalmology 2020; 127:758-66. [PMID: 32085876].

11. Knight LSW, Ruddle JB, Taranath DA, Goldberg I, Smith JEH, Gole G, Chiang MY, Willett F, D'Mellow G, Breen J, Qassim A, Mullany S, Elder JE, Vincent AL, Staffieri SE, Kearns LS, Mackey DA, Luu S, Siggs OM, Souzeau E, Craig JE. Childhood and Early Onset Glaucoma Classification and Genetic Profile in a Large Australasian Disease Registry. Ophthalmology 2021; 128:1549-60. [PMID: 33892047].

12. Cascella R, Strafella C, Germani C, Novelli G, Ricci F, Zampatti S. The genetics and the genomics of primary congenital glaucoma. BioMed Res Int 2015; 1-7

13. Bozkurt B, Yildirim MS, Okka M, Bitirgen G. GAPO syndrome: four new patients with congenital glaucoma and myelinated retinal nerve fiber layer. Am J Med Genet A 2013; 161A:829-34. [PMID: 23494824].

14. Goloni-Bertollo EM, Ruiz MT, Goloni CB, Muniz MP, Valério NI, Pavarino-Bertelli EC. GAPO syndrome: three new Brazilian cases, additional osseous manifestations, and review of the literature. Am J Med Genet A 2008; 146A:1523-9. [PMID: 18470892].

15. Rim PH, Marques-de-Faria AP. Ophthalmic aspects of GAPO syndrome: case report and review. Ophthalmic Genet 2005; 26:143-7. [PMID: 16272061].

16. Gagliardi AR, González CH, Pratesi R. GAPO syndrome: report of three affected brothers. Am J Med Genet 1984; 19:217-23. [PMID: 6507472].

17. Mullaney PB, Jacquemin C, al-Rashed W, Smith W. Growth retardation, alopecia, pseudoanodontia, and optic atrophy (GAPO syndrome) with congenital glaucoma. Arch Ophthalmol 1997; 115:940-1. [PMID: 9230846].

18. Bayram Y, Pehlivan D, Karaca E, Gambin T, Jhangiani SN, Erdin S, Gonzaga-Jauregui C, Wiszniewski W, Muzny D, Elcioglu NH, Yildirim MS, Bozkurt B, Zamani AG, Boerwinkle E, Gibbs RA, Lupski JR. Baylor-Hopkins Center for Mendelian Genomics. Whole exome sequencing identifies three novel mutations in ANTXR1 in families with GAPO syndrome. Am J Med Genet A 2014; 164A:2328-34. [PMID: 25045128].

19. Stránecký V, Hoischen A, Hartmannová H, Zaki MS, Chaudhary A, Zudaire E, Nosková L, Barešová V, Přistoupilová A, Hodaňová K, Sovová J, Hůlková H, Piherová L, Hehir-Kwa JY, de Silva D, Senanayake MP, Farrag S, Zeman J, Martásek P, Baxová A, Afifi HH, St Croix B, Brunner HG, Temtamy S, Kmoch S. Mutations in ANTXR1 cause GAPO syndrome. Am J Hum Genet 2013; 92:792-9. [PMID: 23602711].

20. Wajntal A, Koiffmann CP, Mendonça BB, Epps-Quaglia D, Sotto MN, Rati PB, Opitz JM. GAPO syndrome (McKusick 23074)–a connective tissue disorder: report on two affected sibs and on the pathologic findings in the older. Am J Med Genet 1990; 37:213-23. [PMID: 2248288].

21. Goyal N, Gurjar H, Sharma BS, Tripathi M, Chandra PS. GAPO syndrome with pansutural craniosynostosis leading to intracranial hypertension. BMJ Case Rep 2014; 1-5

22. Ilker SS, Oztürk F, Kurt E, Temel M, Gül D, Sayli BS. Ophthalmic findings in GAPO syndrome. Jpn J Ophthalmol 1999; 43:48-52. [PMID: 10197743].

23. Kocabay G, Mert M. GAPO syndrome associated with dilated cardiomyopathy: an unreported association. Am J Med Genet A 2009; 149A:415-6. [PMID: 19206158].

24. Manouvrier-Hanu S, Largilliere C, Benalioua M, Farriaux JP, Fontaine G. The GAPO syndrome. Am J Med Genet 1987; 26:683-8. [PMID: 3565482].

25. Sayli BS, Gül D. GAPO syndrome in three relatives in a Turkish kindred. Am J Med Genet 1993; 47:342-5. [PMID: 8135278].

26. Quinodoz M, Peter VG, Bedoni N, Royer Bertrand B, Cisarova K, Salmaninejad A, Sepahi N, Rodrigues R, Piran M, Mojarrad M, Pasdar A, Ghanbari Asad A, Sousa AB, Coutinho Santos L, Superti-Furga A, Rivolta C. AutoMap is a high performance homozygosity mapping tool using next-generation sequencing data. Nat Commun 2021; 12:518-1-17[PMID: 33483490].

27. Song Y, DiMaio F, Wang RY, Kim D, Miles C, Brunette T, Thompson J, Baker D. High-resolution comparative modeling with RosettaCM. Structure 2013; 21:1735-42. [PMID: 24035711].

28. García-Castellanos R, Nielsen NS, Runager K, Thøgersen IB, Lukassen MV, Poulsen ET, Goulas T, Enghild JJ, Gomis-Rüth FX. Structural and Functional Implications of Human Transforming Growth Factor β-Induced Protein, TGFBIp, in Corneal Dystrophies. Structure 2017; 25:1740-1750.e2. [PMID: 28988748].

29. Williams CJ, Headd JJ, Moriarty NW, Prisant MG, Videau LL, Deis LN, Verma V, Keedy DA, Hintze BJ, Chen VB, Jain S, Lewis SM, Arendall WB 3rd, Snoeyink J, Adams PD, Lovell SC, Richardson JS, Richardson DC. MolProbity: More and better reference data for improved all-atom structure validation. Protein Sci 2018; 27:293-315. [PMID: 29067766].

30. Van Der Spoel D, Lindahl E, Hess B, Groenhof G, Mark AE, Berendsen HJ. GROMACS: fast, flexible, and free. J Comput Chem 2005; 26:1701-18. [PMID: 16211538].

31. Vanommeslaeghe K, Hatcher E, Acharya C, Kundu S, Zhong S, Shim J, Darian E, Guvench O, Lopes P, Vorobyov I, Mackerell AD Jr. CHARMM general force field: A force field for drug-like molecules compatible with the CHARMM all-atom additive biological force fields. J Comput Chem 2010; 31:671-90. [PMID: 19575467].

32. West MB, Wickham S, Parks EE, Sherry DM, Hanigan MH. Human GGT2 does not autocleave into a functional enzyme: A cautionary tale for interpretation of microarray data on redox signaling. Antioxid Redox Signal 2013; 19:1877-88. [PMID: 23682772].

33. Van Der Meulen KL, Vöcking O, Weaver ML, Meshram NN, Famulski JK. Spatiotemporal Characterization of Anterior Segment Mesenchyme Heterogeneity During Zebrafish Ocular Anterior Segment Development. Front Cell Dev Biol 2020; 8:379-1-16[PMID: 32528955].

34. Lakshminarayanan R, Chaurasia SS, Anandalakshmi V, Chai SM, Murugan E, Vithana EN, Beuerman RW, Mehta JS. Clinical and genetic aspects of the TGFBI-associated corneal dystrophies. Ocul Surf 2014; 12:234-51. [PMID: 25284770].

35. Dighiero P, Drunat S, D'Hermies F, Renard G, Delpech M, Valleix S. A novel variant of granular corneal dystrophy caused by association of 2 mutations in the TGFBI gene-R124L and DeltaT125-DeltaE126. Arch Ophthalmol 2000; 118:814-8. [PMID: 10865320].

36. Klintworth GK, Bao W, Afshari NA. Two mutations in the TGFBI (BIGH3) gene associated with lattice corneal dystrophy in an extensively studied family. Invest Ophthalmol Vis Sci 2004; 45:1382-8. [PMID: 15111592].

37. Pang CP, Fan BJ, Canlas O, Wang DY, Dubois S, Tam PO, Lam DS, Raymond V, Ritch R. A genome-wide scan maps a novel juvenile-onset primary open angle glaucoma locus to chromosome 5q. Mol Vis 2006; 12:85-92. [PMID: 16518310].

38. Liu Y, Munro D, Layfield D, Dellinger A, Walter J, Peterson K, Rickman CB, Allingham RR, Hauser MA. Serial analysis of gene expression (SAGE) in normal human trabecular meshwork. Mol Vis 2011; 17:885-93. [PMID: 21528004].

39. Kim JE, Han MS, Bae YC, Kim HK, Kim TI, Kim EK, Kim IS. Anterior segment dysgenesis after overexpression of transforming growth factor-beta-induced gene, beta igh3, in the mouse eye. Mol Vis 2007; 13:1942-52. [PMID: 17982418].

40. Jiang X, Zhang H. Deterioration of Avellino corneal dystrophy in a Chinese family after LASIK. Int J Ophthalmol 2021; 14:795-9. [PMID: 34150532].

Articles are provided courtesy of Emory University and the Zhongshan Ophthalmic Center, Sun Yat-sen University, P.R. China. The print version of this article was created on 26 December 2023. This reflects all typographical corrections and errata to the article through that date. Details of any changes may be found in the online version of the article.